

**PL-TR-96-2088**

**ANALYZE DATA FROM THE PASP PLUS DOSIMETER  
ON THE APEX SPACECRAFT**

**Frederick A. Hanser  
Paul R. Morel**

**PANAMETRICS, INC.  
221 Crescent Street  
Waltham, MA 02154-3497**

**10 May 1996**

**Final Report**

**July 1993 - April 1996**

**Approved for Public Release; Distribution Unlimited**





**PHILLIPS LABORATORY  
Directorate of Geophysics  
AIR FORCE MATERIEL COMMAND  
HANSCOM AFB, MA 01731-3010**

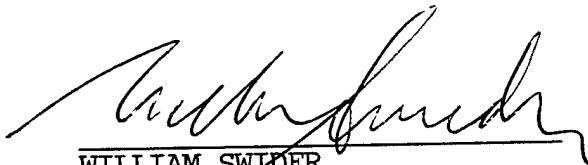
**19960731 102**

**DTIC QUALITY INSPECTED 1**

This technical report has been reviewed and is approved for publication.

  
DONALD A. GUIDICE  
Contract Manager

  
DAVID A. HARDY  
Branch Chief

  
WILLIAM SWIDER  
Deputy Division Director

This report has been reviewed by the ESC Public Affairs Office (PA) and is releasable to the National Technical Information Service (NTIS).

Qualified requestors may obtain additional copies from the Defense Technical Information Center (DTIC). All others should apply to the National Technical Information Service (NTIS).

If your address has changed, or if you wish to be removed from the mailing list, or if the addressee is no longer employed by your organization, please notify PL/IM, 29 Randolph Road, Hanscom AFB, MA 01731-3010. This will assist us in maintaining a current mailing list.

Do not return copies of this report unless contractual obligations or notices on a specific document requires that it be returned.

REPORT DOCUMENTATION PAGE			Form Approved OMB No. 0704-0188	
Public reporting burden for this collection of information is estimated to average 1 hour per response, including the time for reviewing instructions, searching existing data sources, gathering and maintaining the data needed, and completing and reviewing the collection of information. Send comments regarding this burden estimate or any other aspect of this collection of information, including suggestions for reducing this burden, to Washington Headquarters Services, Directorate for Information Operations and Reports, 1215 Jefferson Davis Highway, Suite 1204, Arlington, VA 22202-4302, and to the Office of Management and Budget, Paperwork Reduction Project (0704-0188), Washington, DC 20503.				
1. AGENCY USE ONLY (Leave blank)		2. REPORT DATE 10 May 1996		3. REPORT TYPE AND DATES COVERED Final July 1993 - April 1996
4. TITLE AND SUBTITLE Analyze Data from the PASP Plus Dosimeter on the APEX Spacecraft			5. FUNDING NUMBERS Contract Number: F19628-93-C-0151 PE 63410F PR 2822 TA GC WUPN	
6. AUTHOR(S) Frederick A. Hanser, Paul R. Morel				
7. PERFORMING ORGANIZATION NAME(S) AND ADDRESS(ES) Panametrics, Inc. 221 Crescent Street Waltham, MA 02154-3497			8. PERFORMING ORGANIZATION REPORT NUMBER	
9. SPONSORING/MONITORING AGENCY NAME(S) AND ADDRESS(ES) Phillips Laboratory 29 Randolph Road Hanscom AFB, MA 01731-3010  Contract Monitor: Donald Guidice/GPSG			10. SPONSORING/MONITORING AGENCY REPORT NUMBER PL-TR-96-2088	
11. SUPPLEMENTARY NOTES				
12a. DISTRIBUTION / AVAILABILITY STATEMENT Approved for public release; Distribution unlimited.			12b. DISTRIBUTION CODE	
13. ABSTRACT (Maximum 200 words) Data analysis procedures for the PASP Plus Dosimeter SN/2 in the APEX spacecraft are given, including dead time corrections for high count rate periods. The SN/1 unit calibration data from the MIT Van de Graaff have been reduced to geometric factors, including corrections for the calibration sources. The new calibrated geometric factor electron thresholds deviate slightly the theoretical thresholds and from the earlier calibrations of the CRRES Dosimeter. The PASP Plus Dosimeter electron calibration data are believed to be the more accurate, and are likely to apply to the CRRES D1 detector. The in-orbit data from the SN/2 dosimeter show that all detectors were initially operating properly, and the calibration source data show that the detectors are fully depleted. Typical flux data plots are shown for different orbit orientations. The PASP Plus dosimeter is returning good data from all four domes after 1 year, 9 months in orbit.				
14. SUBJECT TERMS Dosimeter                      Electron Dose                      Proton Dose Electron Flux                  Proton Flux                      Space Radiation			15. NUMBER OF PAGES 36	
			16. PRICE CODE	
17. SECURITY CLASSIFICATION OF REPORT UNCLASSIFIED		18. SECURITY CLASSIFICATION OF THIS PAGE UNCLASSIFIED		19. SECURITY CLASSIFICATION OF ABSTRACT UNCLASSIFIED
				20. LIMITATION OF ABSTRACT UNLIMITED

## Table of Contents

1. Introduction	1
2. PASP Plus Dosimeter Design and Data Reduction	1
2.1 Summary of Dosimeter Design and Operation	1
2.2 Data Analysis and Dead Time Correction	2
3. Electrons Calibration Results from Dosimeter SN/1	8
4. In-Orbit Operational Results from Dosimeter SN/2	18
4.1 General In-Orbit Operation Summary	18
4.2 Calibration Source Data	19
4.3 In-Orbit Dose and Flux Measurements	22
5. Summary and Conclusions	28
References	29

## List of Figures

<u>Figure</u>		<u>Page</u>
1	Isometric View of the PASP Plus Dosimeter	2
2	Dosimeter SN/1 D1A LOLET Channel Calibrated Electron Geometric Factors	11
3	Dosimeter SN/1 D1B LOLET Channel Calibrated Electron Geometric Factors	12
4	Dosimeter SN/1 D2A LOLET Channel Calibrated Electron Geometric Factors	13
5	Dosimeter SN/1 D2B LOLET Channel Calibrated Electron Geometric Factors	14
6	Dosimeter SN/1 D3 LOLET Channel Calibrated Electron Geometric Factors	15
7	Measured Angular Response of D1B LOLET Channel for Electrons	17
8	Measured Angular Response of D2B LOLET Channel for Electrons	17
9	Dosimeter D1A Channel Counts for August 7, 1994	23
10	Dosimeter D2B Channel Counts for August 7, 1994	23
11	Dosimeter D3 Channel Counts for August 7, 1994	24
12	Dosimeter D4 Channel Counts for August 7, 1994	24
13	Dosimeter D1A Channel Counts for November 2, 1994	26
14	Dosimeter D2B Channel Counts for November 2, 1994	26
15	Dosimeter D3 Channel Counts for November 2, 1994	27
16	Dosimeter D4 Channel Counts for November 2, 1994	27

## List of Tables

<u>Table</u>	<u>Page</u>
1 Summary of PASP Plus Dosimeter SN/2 Dome and Detector Properties	3
2 PASP Plus Dosimeter Particle Energy Detection Ranges	3
3 Primary Science Data Entities	4
4 PASP Plus Dosimeter SN/2 Dose Channel Calibration Factors	5
5 PASP Plus Dosimeter SN/2 In-Flight Calibration Source Count Rates	5
6 Approximate Maximum Channel Dead Time Factors for the APEX Orbit	7
7 Dosimeter SN/1 D1A Calibrated Electron Responses	10
8 Dosimeter SN/1 D1B Calibrated Electron Responses	10
9 Dosimeter SN/1 D2A Calibrated Electron Responses	11
10 Dosimeter SN/1 D2B Calibrated Electron Responses	12
11 Dosimeter SN/1 D3 Calibrated Electron Responses	14
12 Calibration Source Data - 8/6/94, 1625 UT	19
13 Calibration Source Data - 9/9/95, 1255 UT	20
14 Calibration Source Data - 12/16/95, 1600 UT	20
15 Calibration Source Data - 1/4/96, 1255 UT	21
16 Calibration Source Data - 1/5/96, 1935 UT	21
17 Average Dose Rates for August 7, 1994	25
18 Average Dose Rates for November 2, 1994	28

## 1. Introduction

The Advanced Photovoltaic and Electronic Experiments (APEX) satellite carries the Photovoltaic Array Space Power Plus Diagnostics (PASP Plus) experiment. PASP Plus includes a Dosimeter to provide a measurement of the particle doses and fluxes behind four thicknesses of aluminum shielding. The PASP Plus Dosimeter design and calibration are described in Reference 1. Two Dosimeters were fabricated to provide a flight unit and a backup unit. Dosimeter SN/2 is on the APEX spacecraft, which was launched on 3 August 1994. The APEX spacecraft and the Dosimeter SN/2 were still operating through April 1996.

A brief summary of the Dosimeter design and data reduction procedures is given in Section 2. More detailed information on the design is given in References 1 and 2. Section 3 contains updated results of electron calibration of the SN/1 Dosimeter at a Van de Graaff accelerator. The LOLET channel results were given in Reference 2, with no corrections for the calibration source background which is small for the LOLET channels. Here, results are also given for the HILETA flux channel, and all data have been corrected for the calibration source background contribution. In-orbit operation is described in Section 4, which includes results up to early 1996.

## 2. PASP Plus Dosimeter Design and Data Reduction

### 2.1 Summary of Dosimeter Design and Operation

The PASP Plus Dosimeter design and operation are described in detail in Reference 1. The dosimeter contains six solid state detectors (SSDs) behind four thicknesses (domes) of aluminum (Al) shielding. The two thinnest Al shields have two SSDs of different areas to allow for a wider dynamic range in incident particle flux. The thinnest dome (D1) is a flat shield of 4.3 mil thick Al, while the other three domes (D2, D3 and D4) are Al hemispheres. The SSDs are shielded from rear entry particles by a 0.5 inch thick tungsten shield, so they have an approximately  $2\pi$  sr FOV. A weak Am-241 calibration source is located behind each SSD to provide a check on SSD gain and total depletion. An isometric view of the Dosimeter is given in Figure 1. Electronic block diagrams and microprocessor program operation are described in References 1 and 2.

The Dosimeter SN/2 is in the APEX PASP Plus payload, with its dome and detector properties being summarized in Table 1. The nominal particle detection energy ranges are summarized in Table 2, and are based on nominal range-energy table calculations. The high energy proton shift from HILET to LOLET is an average of the  $0^\circ$  and  $60^\circ$  energies for D1, and is the  $60^\circ$  energy for D2, D3 and D4. Detailed energy loss curves for the four domes are given in Reference 1. The VHILET energy losses are also given in Table 1, with the count data providing a measure of the proton nuclear "star" production, which is associated with SEUs in sensitive electronic devices.

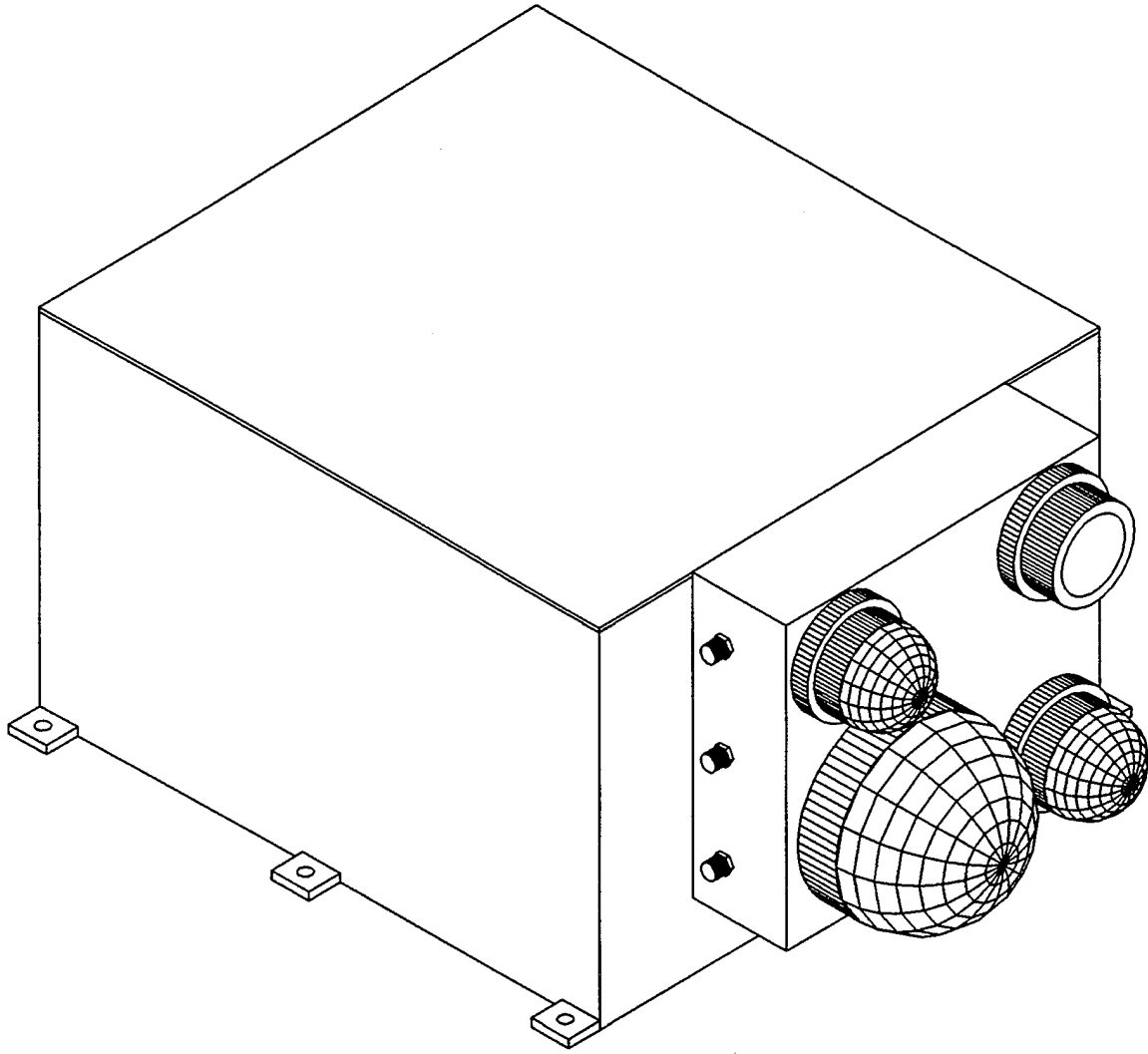


Figure 1. Isometric View of the PASP Plus Dosimeter.

The output data stream provides a set of flux counts and integrated dose counts for the LOLET and HILET channels, and a number of additional counts as listed in Table 3. Normal output provides a set of data for one channel every second, with a complete set for all six channels being obtained every 6 seconds. Details of the command and telemetry operation and formats are given in Reference 1.

## 2.2 Data Analysis and Dead Time Correction

The dosimeter doses are accumulated continuously from turn-on, unless they are reset by command. The accumulated total doses, LOLET and HILET, are calculated from the telemetered data using the dose calibration constants in Table 4. Since the complete dose



counts are output, dose rates can be calculated by taking the difference of successive (6 sec interval) dose counts.

Table 1: Summary of PASP Plus Dosimeter SN/2 Dome and Detector Properties

Dome and Detector No.	Aluminum Shield		Detector		VHILET E Loss (MeV)
	(mils)	(g/cm <sup>2</sup> )	Area (cm <sup>2</sup> ) (A <sub>no,nom</sub> )	Thickness (microns)	
D1/D1A	4.29	0.0294	0.00815	416	40
D1/D1B	4.29	0.0294	0.0514	393	40
D2/D2A	82.5	0.57	0.00815	417	40
D2/D2B	82.5	0.57	0.0514	382	40
D3	232.5	1.59	0.0514	400	40
D4	457.5	3.14	1.000	396	75

Table 2: PASP Plus Dosimeter Particle Energy Detection Ranges

Dome No.	LOLET Particles		HILET Protons (MeV)	VHILET Protons (MeV)
	Electrons (T <sub>n,nom</sub> ) (MeV)	Protons (MeV)		
D1	>0.15	>80	5 - 80	>40
D2	>1.0	>115	20 - 115	>46
D3	>2.5	>120	32 - 120	>56
D4	>5.0	>125	52 - 125	>95

Flux counts can be used with the calibrated geometric factors to provide particle flux data. The flux counts are reset after each readout, so they correspond to 6 second accumulation times. Under conditions of low ambient particle fluxes, the HILETA and HILETB counts can be used to verify SSD gain and total depletion by comparison with the pre-launch calibration source counts. The dosimeter SN/2 calibration source count rates for all channels are listed in Table 5. For periods of low ambient fluxes, the measured dose and flux counts must be corrected for the calibration source count rates to provide true ambient particle dose and flux measurements.

The electron response of the LOLET flux channels for previous dosimeters with identical dome designs was calibrated at accelerators and summarized in References 3 and 4. The energy

dependent electron geometric factors for dome n, in cm<sup>2</sup>-sr, derived from the data in References 3 and 4 are given by the equation

$$\begin{aligned}
 G_{fen}(E) &= 0 & E/T_n &< 1 \\
 &= 7.38 \times A_{no} \times (1 - T_n/E) & 1 \leq E/T_n \leq 3 & \\
 &= 4.92 \times A_{no} & E/T_n \geq 3 &
 \end{aligned}
 \tag{2.1}$$

To first order,  $A_{no}$  is the SSD area  $A_{no,nom}$  from Table 1 and  $T_n = T_{n,nom}$  is the nominal (range/energy calculated) electron threshold energy from Table 2. Actual calibration data change the values of  $A_{no}$  and  $T_n$ , as discussed in Section 3. The proton geometric factors are to first order given by  $\pi \times A_{no}$  cm<sup>2</sup>-sr, with  $A_{no}$  being the SSD area of Table 1. The proton energy responses vary with the angle of incidence because of the change in path length in the SSD sensitive volume, so the ranges in Table 2 are approximate averages, as are the nominal geometric factors.

As discussed in Section 3, the electron calibration data for the PASP Plus dosimeter SN/1 deviate from the  $T_{n,nom}$  values of Table 2 and from the data in References 3 and 4. Thus, the lower energy electron calibrations for the previous dosimeters are questionable. This affects only the absolute electron flux calculations and has no effect on the dose calibrations. Calibrated values for  $T_n$  and  $A_{no}$  are given in Section 3.

Table 3: Primary Science Data Entities

Entity	Mnemonic
Processed 50 keV to 1 MeV Event Count	LOLET COUNT
Processed 1 MeV to 3 MeV Event Count	HILETA COUNT
Processed 3 MeV to 10 MeV Event Count	HILETB COUNT
Processed Digital to Analog Converter Overflow Event Count ( $\geq 10$ MeV)	OVERFLOW COUNT
Very High Energy Deposition Event Count ( $\geq 40$ MeV for D1A, D1B, D2A, D2B and D3) ( $\geq 75$ MeV for D4)	VHILET COUNT
Total Event Count ( $\geq 50$ keV)	TOTAL COUNT
50 keV to 1 MeV Dose	LOLET DOSE
1 MeV to 10 MeV Dose	HILET DOSE

Table 4: PASP Plus Dosimeter SN/2 Dose Channel Calibration Factors

SSD	Area (cm <sup>2</sup> )	Thickness (microns)	LOLET Dose Calibration				HILET Dose Calibration			
			keV Digitizer count	rad TM dose count	Gray TM dose count	keV Digitizer count	rad TM dose count	Gray TM dose count	keV Digitizer count	rad TM dose count
D1A	0.00815	416	37.3	7.57x10 <sup>-7</sup>	7.57x10 <sup>-9</sup>	38.3	6.21x10 <sup>-6</sup>	6.21x10 <sup>-8</sup>	38.3	6.21x10 <sup>-6</sup>
D1B	0.0514	393	38.4	1.306x10 <sup>-7</sup>	1.306x10 <sup>-9</sup>	39.2	1.067x10 <sup>-6</sup>	1.067x10 <sup>-8</sup>	39.2	1.067x10 <sup>-6</sup>
D2A	0.00815	417	38.7	7.83x10 <sup>-7</sup>	7.83x10 <sup>-9</sup>	39.8	6.44x10 <sup>-6</sup>	6.44x10 <sup>-8</sup>	39.8	6.44x10 <sup>-6</sup>
D2B	0.0514	382	39.1	1.369x10 <sup>-7</sup>	1.369x10 <sup>-9</sup>	40.1	1.123x10 <sup>-6</sup>	1.123x10 <sup>-8</sup>	40.1	1.123x10 <sup>-6</sup>
D3	0.0514	400	37.6	1.257x10 <sup>-7</sup>	1.257x10 <sup>-9</sup>	39.1	1.045x10 <sup>-6</sup>	1.045x10 <sup>-8</sup>	39.1	1.045x10 <sup>-6</sup>
D4	1.000	396	39.2	6.81x10 <sup>-9</sup>	6.81x10 <sup>-11</sup>	40.6	5.64x10 <sup>-8</sup>	5.64x10 <sup>-10</sup>	40.6	5.64x10 <sup>-8</sup>

Table 5: PASP Plus Dosimeter SN/2 In-Flight Calibration Source Count Rates

SSD	LOLET Count Rates (cps)			HILET Count Rates (cps)				
	Flux	Dose	HILETA Flux	HILETB Flux	HILETA HILETB	Actual Dose	Telemetered Dose*	
D1A	0.091	0.778	0.137	0.250	0.548	30.4	3.80	
D1B	0.170	2.045	0.487	0.639	0.762	84.0	10.51	
D2A	0.054	0.459	0.082	0.150	0.543	18.1	2.26	
D2B	0.159	1.772	0.802	0.633	1.266	100.6	12.57	
D3	0.087	0.854	0.352	0.591	0.596	72.8	9.10	
D4	0.259	2.024	0.759	0.954	0.796	127.4	15.94	

\* HILET Telemetered Dose = 1/8 HILET Actual Dose

Under normal operation the dosimeter program corrects the data output to telemetry for the microprocessor dead time using the hardware counters for the Total Event Count (Table 3; the method is described in Reference 1). Since the hardware counters for the six Total Event Counts have an electronic dead time of  $0.7 \mu s$ , there is an additional dead time correction which must be applied to all the data when the Total Event Count shows a count rate of about  $10^5/s$  or greater. The correction must be applied to each 6-second readout for the six (6) dosimeter channels (D1A, D1B, D2A, D2B, D3, and D4). The corrections can also be applied to averaged data provided the count rates do not change significantly over the averaging time period.

From Table 3, a complete set of count data for one channel contains the following numbers, all being the count (or average) for a 6 second accumulation period:

Total = the TOTAL COUNT  
 LOflux = the LOLET COUNT  
 HIAflux = the HILETA COUNT  
 HIBflux = the HILETB COUNT  
 OVflux = the OVERFLOW COUNT  
 VHiflux = the VHILET COUNT  
 LOdose = the LOLET DOSE  
 HIDose = the HILET DOSE

There are two factors that are needed. The first factor applies only to the flux counts, while the second factor applies to both the flux and delta-dose counts. The dead time factors are calculated from the TM counts, or averages, by

$$DTF_{flux} = Total / (LOflux + HIAflux + HIBflux + OVflux) \quad (2.2)$$

and

$$DTF_{flux,dose} = 1 / (1 - Total \times 0.7 \times 10^{-6} / 6). \quad (2.3)$$

The  $DTF_{flux}$  factor of (2.2) is the effective microprocessor dead time, and the microprocessor has already applied this factor to the Dose Counts (LOLET DOSE and HILET DOSE; see Reference 1). The  $DTF_{flux,dose}$  factor of (2.3) is the dead time associated with the TOTAL COUNT (hardware dead time), and must be applied to all data counts, except for the VHILET COUNT, which is a separate hardware counter.

The dead time corrected Total count is obtained from

$$Total_{corr} = Total \times DTF_{flux,dose}, \quad (2.4)$$

while the dead time corrected Flux counts (LOflux, HIAflux, HIBflux, and OVflux) are obtained from

$$Flux_{corr} = Flux \times DTF_{flux} \times DTF_{flux,dose}. \quad (2.5)$$

As noted above, there is no correction for the VHiflux counts.

The dose counts (LOdose and HIdose) must have the delta doses corrected by

$$\Delta Dose_{corr} = \Delta Dose \times DTF_{flux, dose} \quad (2.6)$$

where

$$\Delta Dose = Dose(\text{present readout}) - Dose(\text{previous readout}). \quad (2.7)$$

Note that the  $\Delta Dose$  values correspond to either 6 seconds (for single readouts) or to the averaging time period (for averaged data), while the flux (or average flux) counts always correspond to a 6 second accumulation interval.

The dead-time factors are generally important only at the peak count-rate periods of the inner radiation belt, where the maximum count rates are measured. The approximate maximum factors are illustrated by data from August 5, 1994, at about 0630 UT. The measured maximum counts and the corresponding factors  $DTF_{flux}$  and  $DTF_{flux, dose}$  are listed in Table 6. From Table 6 it can be seen that  $DTF_{flux}$  is important for D1A, D1B, and D4, while  $DTF_{flux, dose}$  is only important for D1A and D1B. Thus, the  $\Delta Dose$  corrections of (2.6) need be made only for D1A and D1B. A survey of several orbits over the period of early August 1994 through late September 1994 shows that the above listed maximum Total counts are never exceeded by a significant amount, so Table 6 lists the expected maximum dead time factors for the dosimeter in the APEX orbit.

Note that the corrected  $\Delta Dose$  values must be summed to provide a corrected total dose for each orbit. These corrected total dose values must be used to obtain the true dose exposure of each channel. The total dose corrections are important only during the time of the peak inner-belt count rates, and are only important for the D1A and D1B channels.

Table 6: Approximate Maximum Channel Dead Time Factors for the APEX Orbit

Channel	Total Count (6 seconds)	$DTF_{flux}$ (Eq. (2.2))	$DTF_{flux, dose}$ (Eq. (2.3))
D1A	$1.44 \times 10^6$	7.77	1.136
D1B	$4.51 \times 10^6$	24.29	1.602
D2A	$1.91 \times 10^3$	1.08	1.0002
D2B	$7.13 \times 10^3$	1.025	1.0006
D3	$5.65 \times 10^3$	1.020	1.0005
D4	$7.75 \times 10^3$	1.275	1.0006

### 3. Electron Calibration Results from Dosimeter SN/1

The geometry of the calibration set-up at the MIT Van de Graaff and the details of the data analysis method are given in Reference 2. Reference 2 only presented the results for the LOLET channels, and made no correction for the background counts of the calibration sources. These calculations have been updated to correct for the calibration source background, which is small for the LOLET channels, and to include the geometric factors for the HILETA flux channel. The HILETA channels have a small but non-zero response for electrons, so they are presented here. The analysis of Reference 2 is changed only in that the counts used in Eqs. (3.2) and (3.3) of Reference 2 have the value of "cnt(Di)" changed to "cnt(Di) - cnt(cal source, Di)". The resulting geometric factors are summarized in Tables 7 to 11 for the five channels which could be calibrated.

The calibration results for the Dosimeter SN/1 D1 dome, channels D1A and D1B, are given in Tables 7 and 8. The LOLET geometric factors are plotted in Figures 2 and 3, where they are compared with the nominal fit from Eq. (2.1) and a calibrated fit using modified values for  $T_n$  and  $A_{no}$ . Since the D1 dome is a flat Al shield and not a hemisphere, the fit of Eq. (2.1) which was derived from hemispherical shield calibration data (References 3 and 4) does not necessarily apply. However, the D1A fit is quite good, while the D1B fit shows some deviations primarily because of the fast rise and high energy fall-off of the calibration data. The calibrated fits to the D1A and D1B geometric factors are acceptable within the accuracy of the calibration data. The calibrated  $T_n$  value is about 25% higher than the nominal value calculated from the range/energy thickness of the Al foil (0.13 MeV) plus the need for a 50 keV energy loss in the detector to trigger the lowest threshold (incident electron energy must be 0.15 MeV =  $T_{n,nom}$ ).

The average measured values of  $A(0^\circ)$  for energies above 0.5 MeV are 0.0150 cm<sup>2</sup> for D1A and 0.0790 cm<sup>2</sup> for D1B, while the actual detector areas are 0.00815 cm<sup>2</sup> and 0.0514 cm<sup>2</sup>. The difference is an effect of the scattering of the electrons in the SSD, as discussed in Reference 4. The effective value of  $A_{no}$  is better given as:

$$A_{no,eff} = A_{no} + \pi \times d \times t, \quad (3.1)$$

where  $A_{no}$  is the area of the sensitive volume of the detector (Table 1),  $d$  is the diameter of  $A_{no}$ , and  $t$  is the detector thickness. This effect is largest for the smallest area SSDs, where the diameter  $d$  is only a few times the thickness  $t$ . For D1A (3.1) gives

$$A_{no,eff} = 0.00815 + \pi \times 0.1019 \times 0.04 = 0.0210 \text{ cm}^2 \quad (3.2)$$

and for D1B it gives

$$A_{no,eff} = 0.0514 + \pi \times 0.2558 \times 0.04 = 0.0835 \text{ cm}^2. \quad (3.3)$$

For the D1 dome the calibrated  $A_{no}$  values used for the fit of (2.1) are expected to differ somewhat from the measured detector values since the Al shield is flat while the fit of (2.1) is based on a hemispherical shield. The best fit values of  $A_{no}$  used in (2.1) are 0.0090 cm<sup>2</sup> for D1A and 0.044 cm<sup>2</sup> for D1B, which are about half of the measured  $A(0^\circ)$  values.

The HILETA calibration data for the D1A channel are all less than about 10<sup>-5</sup> cm<sup>2</sup> for the  $A(0^\circ)$  and 10<sup>-5</sup> cm<sup>2</sup>sr for the geometric factor, which values are upper limits from the count subtraction statistics. The D1B calibration data give reasonable HILETA calibration data above about 1 MeV, which is the HILETA threshold energy loss. Statistical accuracy is about 10<sup>-5</sup> for both the  $A(0^\circ)$  and the geometric factor, so the 0.896 MeV point is at the limit of the statistical accuracy. Since the average electron energy is less than the 1 MeV threshold for the HILETA channel, the non-zero geometric factor for the 0.896 MeV point is partly the result of the electron beam energy spread through the Van de Graaff exit window and the air path to the Dosimeter, and statistical fluctuations in the energy loss in the Al shield foil.

The calibration results for the Dosimeter SN/1 D2 dome, channels D2A and D2B, are given in Tables 9 and 10, and plotted in Figures 4 and 5. The D2A channel is identical to the D1 channel of the CRRES dosimeter (Reference 4), so the CRRES D1 calibration data and Gf fit are also plotted in Figure 4. The CRRES D1 Gf fit requires a value of  $A_{no} = 0.01744$  cm<sup>2</sup>, which is about twice the nominal area of 0.00815 cm<sup>2</sup>, but is close to the D1A measured value of 0.0150 cm<sup>2</sup> for  $A(0^\circ)$  and to the corrected value of (3.2). The CRRES calibration fit has  $T_n = 1.0$  MeV, while the PASP Plus D2A data give  $T_n = 1.8$  MeV. The PASP Plus D2A fit has used  $T_n = 1.5$  MeV and  $A_{no} = 0.01744$  cm<sup>2</sup> to give a slightly better fit at the high-energy region.

The D2B Gf data in Figure 5 are compared with the Gf fit of Eq. (2.1) using a nominal value of  $A_{no} = 0.0514$  cm<sup>2</sup>, and also using a calibrated fit with  $T_n = 1.5$  MeV and  $A_{no} = 0.080$  cm<sup>2</sup>, which latter value is in agreement with the calibrated values of Reference 4. Eq. (3.3) gives  $A_{no,eff} = 0.0835$  cm<sup>2</sup> while the D1B data give  $A(0^\circ) = 0.079$  cm<sup>2</sup>. Since the MIT Van de Graaff limits near 3.5 MeV, the high energy limit of Gf for the PASP Plus dosimeter D2 dome was not reached. The PASP Plus D2B data give a calibrated fit of  $T_n = 1.9$  MeV, but a fit using  $T_n = 1.5$  MeV provides a better high-energy fit.

The calibration results for the Dosimeter SN/1 D3 dome/channel are given in Table 11, and plotted in Figure 6. The D3 channel is identical to the D2 channel of the CRRES dosimeter (Reference 4), so the CRRES D2 calibration data and nominal Gf fit are also plotted in Figure 6. The CRRES D2 Gf fit required a value  $A_{no} = 0.075$  cm<sup>2</sup> (Reference 4), while Eq. (3.3) gives  $A_{no,eff} = 0.0835$  cm<sup>2</sup>, which is reasonable agreement. The PASP Plus dosimeter D3 calibration data only show the very beginning of the rise in Gf, but it appears to be in reasonable agreement with the CRRES D2 Gf calibration data. The measured CRRES D2 Gf half-height energy is

Table 7: Dosimeter SN/1 D1A Calibrated Electron Responses

Effective Electron Beam Energy (MeV)	LOLET Calibration		HILETA Calibration	
	Area (0°) (10 <sup>-2</sup> cm <sup>2</sup> )	G Factor (10 <sup>-2</sup> cm <sup>2</sup> sr)	Area (0°) (10 <sup>-2</sup> cm <sup>2</sup> )	G Factor (10 <sup>-2</sup> cm <sup>2</sup> sr)
0.169	0.00095	0.0179	-	-
0.225	0.340	0.829	-	-
0.328	1.249	3.02	-	-
0.428	1.582	3.88	-	-
0.665	1.674	4.36	-	-
0.896	1.566	4.45	<0.001	<0.001
1.125	1.586	4.38	<0.001	<0.001
1.352	1.476	4.32	<0.001	<0.001
1.579	1.361	4.23	<0.001	<0.001
1.807	1.344	4.38	<0.001	<0.001
2.260	1.481	4.89	<0.001	<0.001

Table 8: Dosimeter SN/1 D1B Calibrated Electron Responses

Effective Electron Beam Energy (MeV)	LOLET Calibration		HILETA Calibration	
	Area (0°) (10 <sup>-2</sup> cm <sup>2</sup> )	G Factor (10 <sup>-2</sup> cm <sup>2</sup> sr)	Area (0°) (10 <sup>-2</sup> cm <sup>2</sup> )	G Factor (10 <sup>-2</sup> cm <sup>2</sup> sr)
0.169	0.0690	0.0128	-	-
0.225	2.35	5.58	-	-
0.328	7.63	18.79	-	-
0.428	8.80	22.15	-	-
0.665	8.64	21.05	-	-
0.896	8.18	20.36	0.00053	0.0026
1.125	8.24	19.67	0.0199	0.093
1.352	8.02	19.15	0.0132	0.054
1.579	7.61	18.71	0.0101	0.053
1.807	7.54	19.06	0.0091	0.061
2.260	7.04	18.49	0.0062	0.041



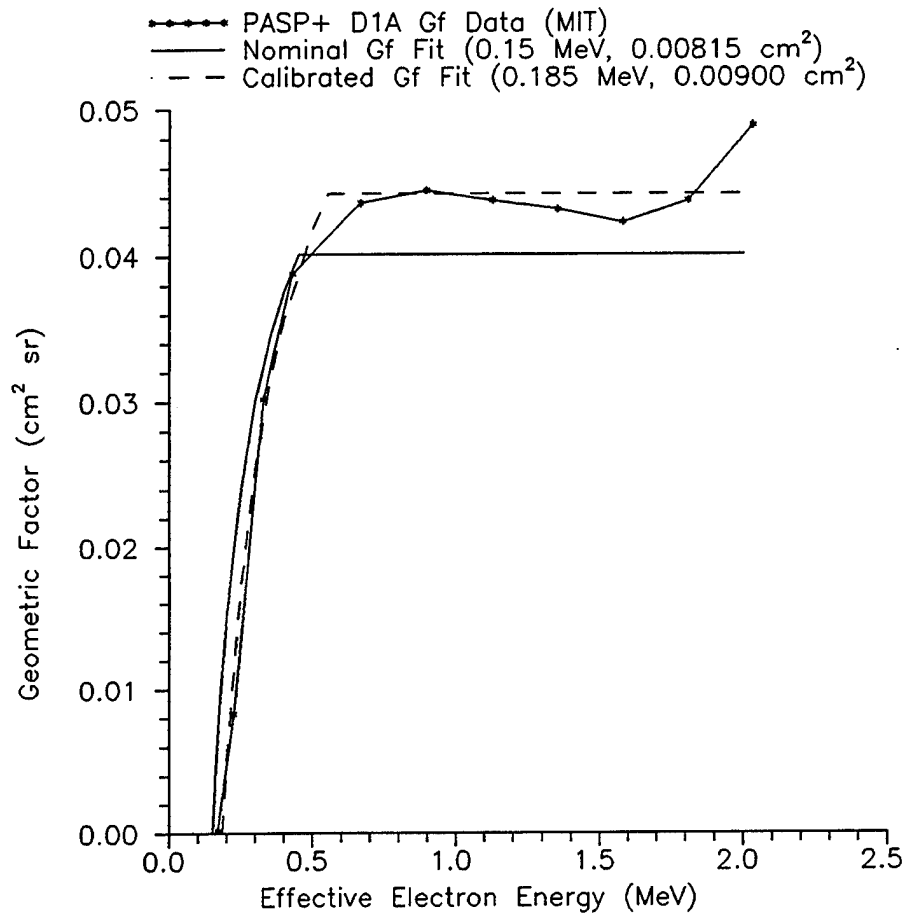


Figure 2. Dosimeter SN/1 D1A LOLET Channel Calibrated Electron Geometric Factors.

Table 9: Dosimeter SN/1 D2A Calibrated Electron Responses

Effective Electron Beam Energy (MeV)	LOLET Calibration		HILETA Calibration	
	Area (0°) (10 <sup>-2</sup> cm <sup>2</sup> )	G Factor (10 <sup>-2</sup> cm <sup>2</sup> sr)	Area (0°) (10 <sup>-2</sup> cm <sup>2</sup> )	G Factor (10 <sup>-2</sup> cm <sup>2</sup> sr)
1.125	0.0015	0.0081	-	-
1.352	0.0477	0.163	-	-
1.579	0.150	0.634	-	-
1.807	0.283	1.192	-	-
2.033	0.419	1.710	-	-
2.260	0.561	2.313	<0.0001	<0.0005
2.487	0.702	3.01	0.0001	0.00066
2.713	0.963	4.16	<0.0001	0.00127
2.940	1.552	6.26	<0.0001	0.00100

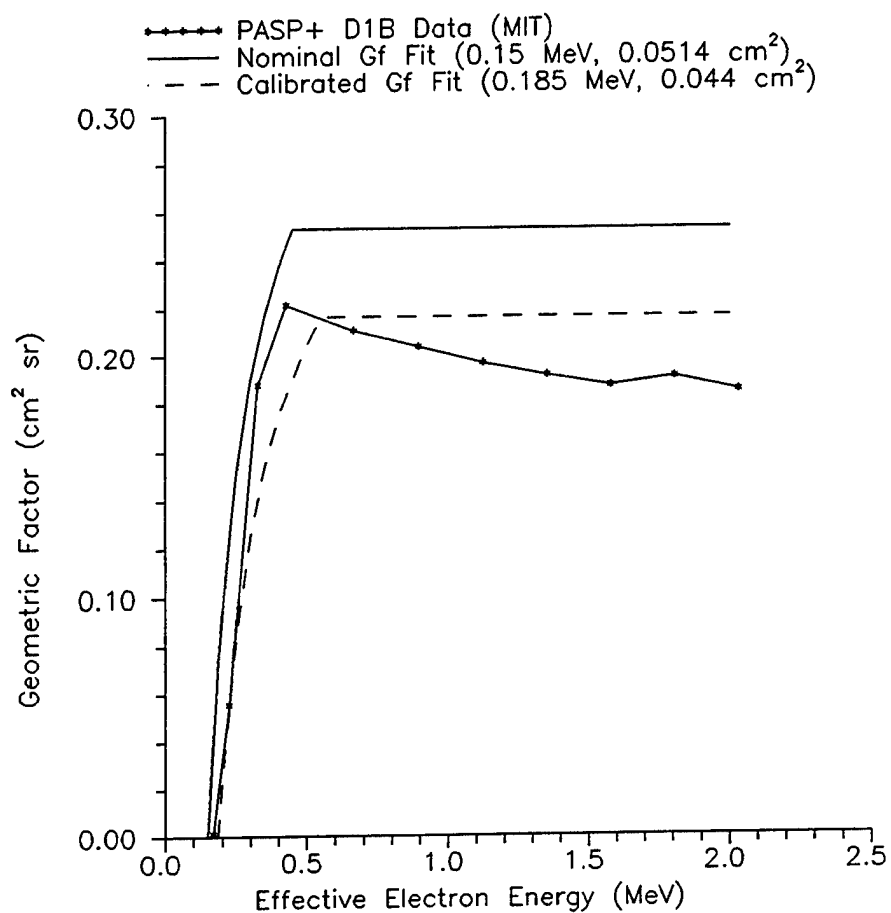


Figure 3. Dosimeter SN/1 D1B LOLET Channel Calibrated Electron Geometric Factors.

Table 10: Dosimeter SN/1 D2B Calibrated Electron Responses

Effective Electron Beam Energy (MeV)	LOLET Calibration		HILETA Calibration	
	Area(0°) (10 <sup>-2</sup> cm <sup>2</sup> )	G Factor (10 <sup>-2</sup> cm <sup>2</sup> sr)	Area(0°) (10 <sup>-2</sup> cm <sup>2</sup> )	G Factor (10 <sup>-2</sup> cm <sup>2</sup> sr)
1.125	0.0139	0.0547	-	-
1.352	0.261	1.052	-	-
1.579	0.835	3.56	<0.001	<0.001
1.807	1.534	6.71	0.00102	0.0064
2.033	2.209	9.22	0.00239	0.0132
2.260	2.91	11.90	0.00447	0.0267
2.487	3.60	14.44	0.00647	0.0327
2.713	4.29	17.60	0.00645	0.0364
2.940	5.39	22.30	0.0102	0.0499

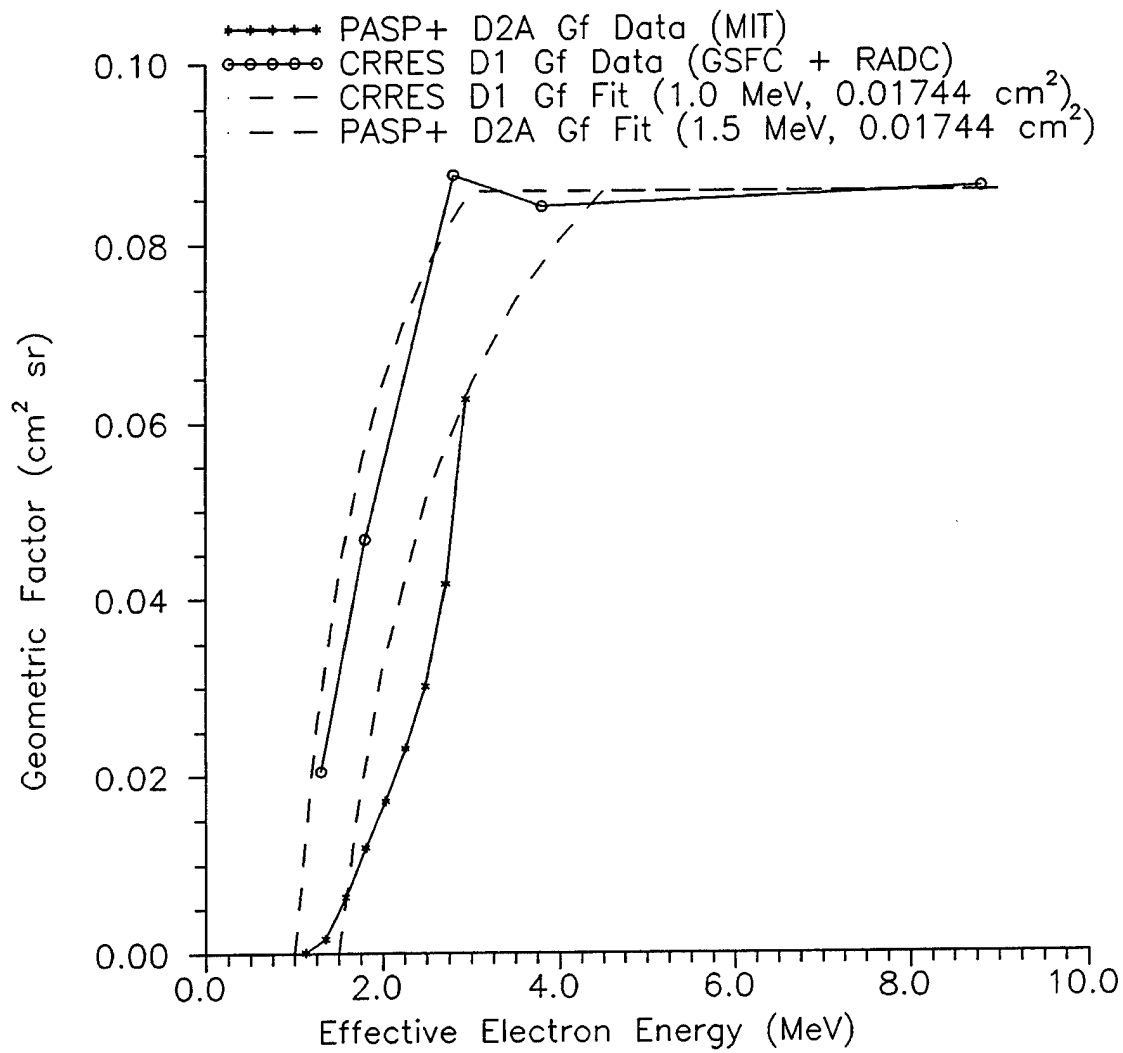


Figure 4. Dosimeter SN/1 D2A LOLET Channel Calibrated Electron Geometric Factors.

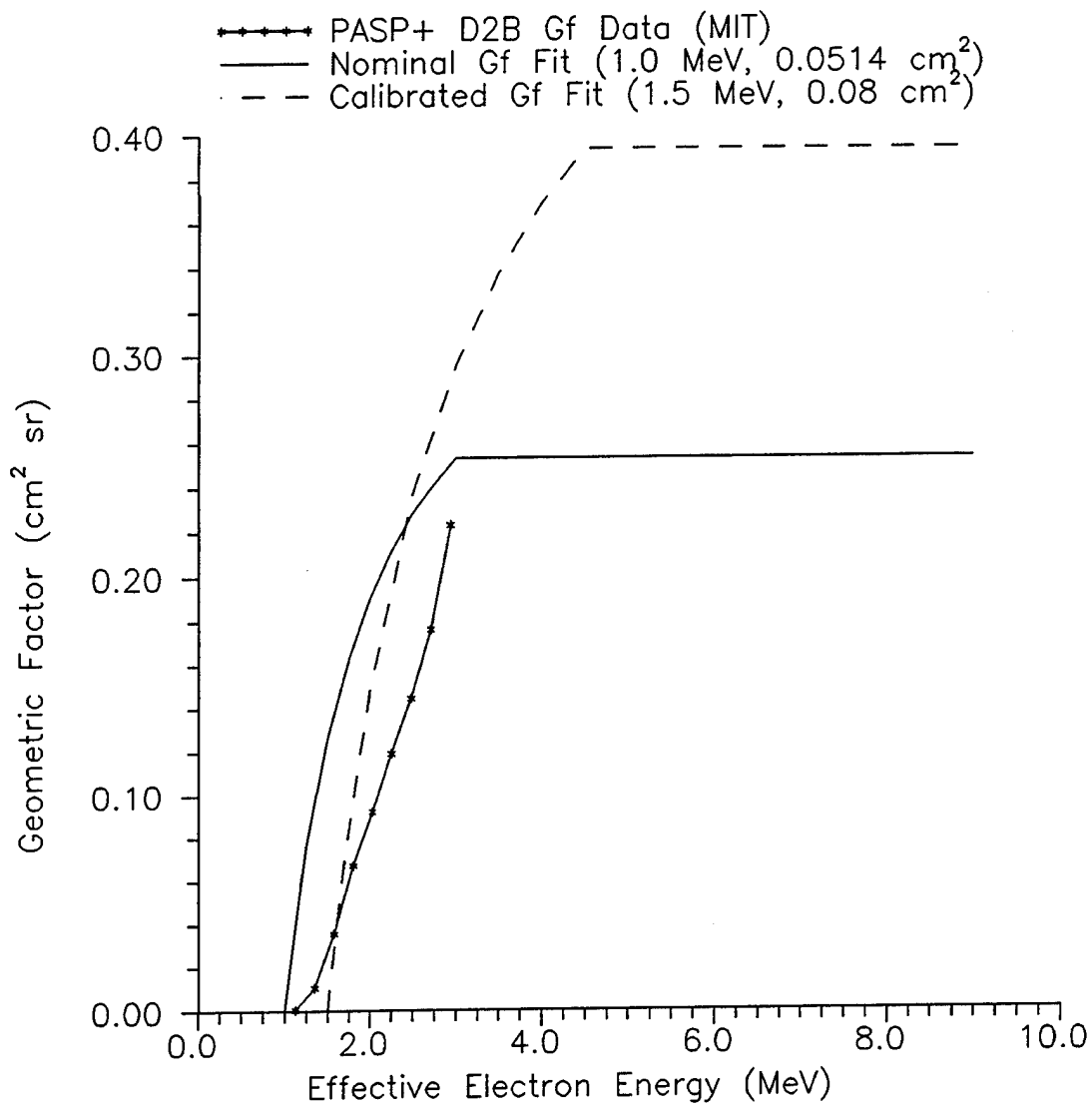


Figure 5. Dosimeter SN/1 D2B LOLET Channel Calibrated Electron Geometric Factors.

Table 11: Dosimeter SN/1 D3 Calibrated Electron Responses

Effective Electron Beam Energy (MeV)	LOLET Calibration		HILETA Calibration	
	Area(0°) (10 <sup>-2</sup> cm <sup>2</sup> )	G Factor (10 <sup>-2</sup> cm <sup>2</sup> sr)	Area(0°) (10 <sup>-2</sup> cm <sup>2</sup> )	G Factor (10 <sup>-2</sup> cm <sup>2</sup> sr)
2.260	0.00336	0.0269	<0.0003	0.00151
2.487	0.00489	0.0639	<0.0003	0.00095
2.713	0.0133	0.1268	<0.0003	0.00121
2.940	0.0809	0.463	<0.0003	0.00131
3.076	0.1387	0.967	<0.0003	<0.001

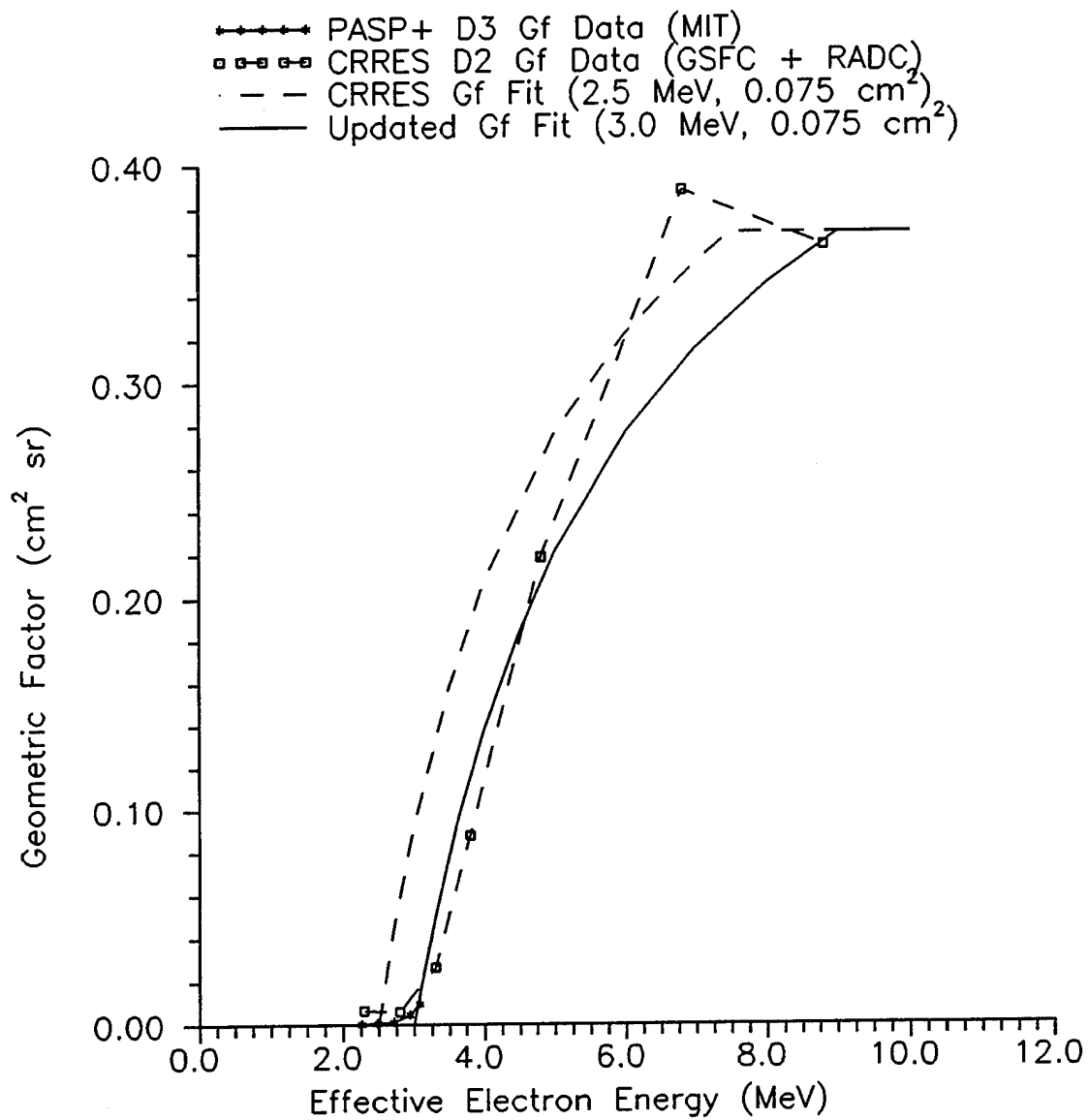


Figure 6. Dosimeter SN/1 D3 LOLET Channel Calibrated Electron Geometric Factors.

about 4.5 MeV, about 1.2 times the nominal Gf fit half-height energy of 3.75 MeV (fit  $T_n = 3.0$  MeV, nominal  $T_n = 2.5$  MeV).

The dosimeter electron response fit in Eq. (2.1) was generated from the DMSP/F7 dosimeter calibration data (Reference 3), which was most reliable for the highest energies (above about 4 MeV). The CRRES dosimeter was calibrated at lower electron energies at both the NASA/GSFC Van de Graaff, and at the RADC Linear Accelerator (Linac; Reference 4). The GSFC calibrations covered only the electron energies below about 1.8 MeV, and provided only a comparatively small area electron beam (about 0.25 inch diameter). Also, the GSFC beam monitor measured intensity only before and after each dosimeter measurement, and there is some question of the beam energy calibration.

The low-energy electron calibration of the CRRES dosimeter at the RADC Linac suffered from a weak beam intensity and a large energy spread in the beam. The lowest energy channel electron response, i.e. the D1 dome on the CRRES and DMSP/F7 dosimeters, is thus somewhat uncertain, and it is felt that the detailed calibration measurements made with the PASP Plus dosimeter at the MIT Van de Graaff are the more accurate. The PASP Plus dosimeter gives a fit  $T_n$  value about 25% larger than the nominal  $T_n$  energy for the D1 dome ( $T_{n,nom} = 0.15$  MeV), and a fit  $T_n$  value about 50% larger than the nominal  $T_n$  energy for the D2 dome ( $T_{n,nom} = 1.0$  MeV). The fit  $T_n$  value is about 20% larger than the nominal  $T_n$  energy for the D3 dome ( $T_{n,nom} = 2.5$  MeV). It is expected that the fit of Eq. (2.1) should be quite good for the highest energy D4 dome ( $T_{n,nom} = 5.0$  MeV), using  $T_n = 5.0$  MeV and  $A_{no} = 1.00$  cm<sup>2</sup>.

The measured angular responses of the PASP Plus dosimeter are summarized by the plots in Figures 7 and 8. Figure 7 shows the angular response of the D1B channel for electrons of 0.328, 1.125 and 2.037 MeV energy. A  $\cos(\theta)$  curve is also plotted, and shows reasonable agreement up to at least 60°. Use of a full  $\cos(\theta)$  fit out to 90° gives a reasonable approximation for the full Gf value. The measured angular response is in reasonable agreement with that expected for the flat shield of the D1 dome.

The D2B channel angular responses for electrons of 1.579, 2.260 and 2.940 MeV energy are shown in Figure 8. The plotted fit is for

$$(A_n(\theta)/A_n(0))_{fit} = (2 + 3 \times \cos(\theta))/5 \quad (3.4)$$

which was found for the earlier dosimeter dome calibrations (References 3, 4), and provides a reasonable fit to the new measurements. The D3 and D4 domes are expected to have similar electron angular responses.

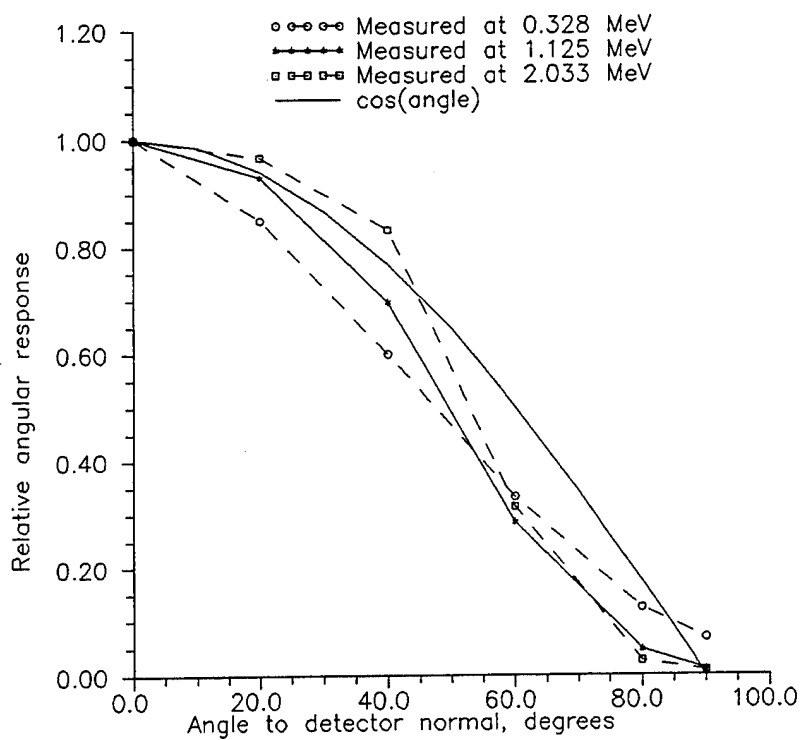


Figure 7. Measured Angular Response of D1B LOLET Channel for Electrons.

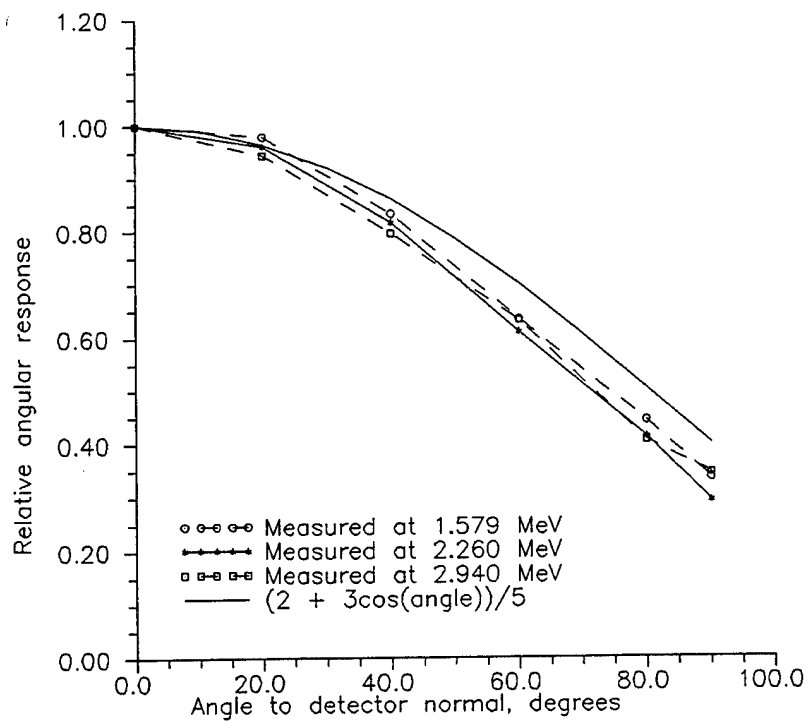


Figure 8. Measured Angular Response of D2B LOLET Channel for Electrons.

#### 4. In-Orbit Operational Results from Dosimeter SN/2

##### 4.1 General In-Orbit Operation Summary

Following the APEX spacecraft launch at about 1430 UT on August 3, 1994, the PASP Plus dosimeter was turned on at about 0410 UT on August 5, 1994. Initial dosimeter operation showed proper operation of all electronics and detectors, with total detector depletion and proper electronic gains being verified by calibration source data (see Section 4.2). Since turn on, the dosimeter has operated continually to the extent allowed by spacecraft conditions. The dosimeter has been on continuously, except for a period from mid-November 1994 to early January 1995 and for a second period from mid-September 1995 to mid-December 1995, when there were spacecraft control problems. The dosimeter is still operating as of April 1996.

The D1A detector showed increased noise levels after about 3 weeks of operation, with some noise burst being observed beginning about August 25, 1994. Noisy behavior ended about October 12, 1994, but began again after dosimeter turn on in January 1995. By mid-February 1995 the D1A noise had stopped. Thereafter, the D1A detector showed some noise bursts in early July 1995, but appeared to be mostly noise-free until turn off in mid-September 1995. Following turn on in mid-December 1995, the D1A detector has shown progressively worse noise output. The D1B detector has operated properly for the entire time that the dosimeter has been on, and the dead time corrected data provide all the information required for the D1 dome dose measurements.

During some periods of the APEX spacecraft operations power limitations resulted in the dosimeter operating at low temperatures. During some periods the dosimeter was cycled on and off as a power conserving measure, and the detector temperatures reached -5°C and less. The most notable periods of low temperature operation were in late May 1995. At this time the D1B bias voltage monitor showed a low reading, dropping to 105 V (nominal is 150 V) at -5°C. This indicates a low temperature problem with the bias voltage regulator circuit for the D1B detector, which shows up only below about 5°C. This could be the result of radiation degradation of a marginal component, since pre-launch tests to -30°C showed no problems with any of the detector bias voltage circuits. Checks of the D1B calibration source data show that the detector is still totally depleted at 105 V, so no data was lost during the low temperature operation periods.

The dosimeter data have been checked periodically to verify proper operation. No analog or digital monitors have shown any anomaly, other than the D1B bias voltage below 5°C. All microprocessor error flags and error counts have remained at 0. In late April 1996, after 1 year 9 months in orbit, the PASP Plus dosimeter is still operating properly, with only the D1A detector showing degraded operation. All four (4) domes are still supplying dose information.



## 4.2 Calibration Source Data

The calibration source behind each detector provides a minimum count rate which is usually observable during the perigee part of each APEX orbit. The HILETA and HILETB flux channel count rates come from the degraded peak energy (about 3 MeV) of the calibration alpha particle source ( $^{241}\text{Am}$ , undegraded peak = 5.48 MeV), which only penetrates about 15 microns into the rear surface of the detectors. Since the detectors are 400 microns thick, measurement of the alpha source can verify detector depletion to within a few microns as well as proper gain. The pre-launch count rates for the PASP Plus dosimeter SN/2 are listed in Table 5, and are the base count rates used to verify total depletion of the solid state detectors and stability of the electronic gains.

Calibration source data taken shortly after the PASP Plus dosimeter was turned on in orbit are shown in Table 12, where the measured LOLET, HILETA and HILETB flux count rates are given along with the ratios to the pre-launch calibration source values. The HILETA and HILETB fluxes are in good agreement with the pre-launch baseline count rates, and verify that the detectors are totally depleted and the electronic gains have not changed. The LOLET fluxes are all higher than the pre-launch calibration source values, but this is the result of an ambient low energy particle flux. Bremsstrahlung from electrons above 50 keV could be the dominant source.

Table 12: Calibration Source Data - 8/6/94, 1625 UT

Channel	LOLET Flux		HILETA Flux		HILETB Flux	
	Meas (cps)	<u>Meas</u> Base	Meas (cps)	<u>Meas</u> Base	Meas (cps)	<u>Meas</u> Base
D1A	0.143	1.58	0.140	1.02	0.225	0.90
D1B	0.558	3.27	0.496	1.02	0.694	1.09
D2A	0.112	2.09	0.089	1.09	0.159	1.06
D2B	0.318	2.00	0.760	0.95	0.721	1.14
D3	0.174	2.00	0.291	0.83	0.547	0.93
D4	1.248	4.81	0.880	1.16	1.058	1.11

Calibration source data from September 9, 1995, shortly before the dosimeter was turned off for a few months, and after more than a year in orbit, are shown in Table 13. The HILETA and HILETB flux count rates are all in good agreement with the pre-launch values, except for D1A which is slightly low. The D1A HILETA flux count rate is based on a sum of only 56 counts, which gives a statistical error standard deviation of 13%, so within statistics D1A is still operating properly.

Table 13: Calibration Source Data - 9/9/95, 1255 UT

Channel	LOLET Flux		HILETA Flux		HILETB Flux	
	Meas (cps)	<u>Meas</u> Base	Meas (cps)	<u>Meas</u> Base	Meas (cps)	<u>Meas</u> Base
D1A	0.180	1.98	0.067	0.49	0.193	0.77
D1B	0.419	2.46	0.486	1.00	0.686	1.07
D2A	0.081	1.51	0.085	1.04	0.171	1.14
D2B	0.251	1.58	0.716	0.89	0.711	1.12
D3	0.141	1.62	0.329	0.93	0.588	0.99
D4	0.778	3.00	0.725	0.96	0.961	1.01

The PASP Plus Dosimeter was turned off in mid-September 1995 because of spacecraft control problems, and was not turned on again until mid-December 1995. Following the December 1995 turn-on the D1A SSD was very noisy and never recovered. The perigee calibration source data show that the D1B SSD was not operating in a totally depleted mode from mid-December 1995 to January 5, 1996. Calibration source data from shortly after dosimeter turn-on are shown in Table 14. The D1B HILETA and HILETB flux count rates are much below the calibration source values, with the LOLET flux count rate being the approximate sum of the three channels. This continued to January 4, 1996, and on January 5, 1996 the D1B detector appears to have completely recovered. Calibration source data for January 4 and 5 1996 are shown in Tables 15 and 16. Note that Table 16 indicates that the D1A detector was also operating properly during that particular perigee, but the detector showed large noise count rates during much of this time, so the D1A data from this time period are not reliable.

Table 14: Calibration Source Data - 12/16/95, 1600 UT

Channel	LOLET Flux		HILETA Flux		HILETB Flux	
	Meas (cps)	<u>Meas</u> Base	Meas (cps)	<u>Meas</u> Base	Meas (cps)	<u>Meas</u> Base
D1A	(noise)	-	0.000	0.00	0.000	0.00
D1B	1.591	9.34	0.000	0.00	0.000	0.00
D2A	0.068	1.27	0.100	1.23	0.145	0.97
D2B	0.255	1.60	0.704	0.88	0.772	1.22
D3	0.167	1.92	0.313	0.89	0.581	0.98
D4	1.196	4.61	0.736	0.97	1.037	1.09

Table 15: Calibration Source Data - 1/4/96, 1255 UT

Channel	LOLET Flux		HILETA Flux		HILETB Flux	
	Meas (cps)	<u>Meas</u> Base	Meas (cps)	<u>Meas</u> Base	Meas (cps)	<u>Meas</u> Base
D1A	(noise)	-	0.000	0.00	0.000	0.00
D1B	1.557	9.14	0.000	0.00	0.000	0.00
D2A	0.080	1.49	0.111	1.36	0.155	1.03
D2B	0.251	1.58	0.695	0.87	0.768	1.21
D3	0.165	1.90	0.336	0.95	0.560	0.95
D4	1.158	4.47	0.749	0.99	1.048	1.10

Table 16: Calibration Source Data - 1/5/96, 1935 UT

Channel	LOLET Flux		HILETA Flux		HILETB Flux	
	Meas (cps)	<u>Meas</u> Base	Meas (cps)	<u>Meas</u> Base	Meas (cps)	<u>Meas</u> Base
D1A	0.437	4.82	0.127	0.93	0.243	0.97
D1B	0.306	1.80	0.520	1.07	0.703	1.10
D2A	0.073	1.36	0.094	1.15	0.145	0.97
D2B	0.199	1.25	0.691	0.86	0.833	1.32
D3	0.135	1.55	0.323	0.92	0.511	0.86
D4	1.184	4.57	0.679	0.89	1.034	1.08

The D1B SSD response after the December 1995 turn-on indicates a partially depleted SSD, since the calibration source is not seen in the HILETA and HILETB channels, and the response to inner belt protons is strongly reduced. Over the period of January 4 to 5 1996 the D1B SSD becomes totally depleted, and response to both the calibration source and to radiation belt protons returns to normal. The explanation for this is not clear, but may lie in the intense irradiation received while unbiased.

The D1B SSD accumulated a substantial flux of low energy electrons and protons during the unbiased period from September 1995 to December 1995. Possibly this irradiation produced a thin layer of very low resistivity silicon near the front surface, and when bias was reapplied in December 1995 the bias voltage of 150 V was not sufficient to provide total depletion. Over the next few weeks the D1B SSD slowly "healed" the radiation damage, and the low resistivity layer of silicon returned to a higher resistivity value as the impurity (doping element) distribution returned to the earlier (uniform) distribution. The dosimeter SSDs are pin

photodiodes, which use doped layers of silicon to provide the rectifying junction that produces a depletion region. The observed phenomenon is interesting, in that the unbiased SSD is affected by intense low energy particle fluxes, but then can recover after bias is reapplied. Note that the D2A, D2B, D3 and D4 SSDs showed no such degradation, but they are shielded by at least 0.57 g/cm<sup>2</sup> of aluminum. It is not clear if the D1B damage/recovery observed was caused by low energy particle fluxes, or simply by the fact that the particle flux exposure was more intense.

The noisy character of the D1A SSD is similar to what has been observed earlier, where the SSD becomes noisy when left without bias voltage applied for a day or more. Under these conditions the D1A SSD recovers after a week or two under bias. Following the December 1995 turn-on, the D1A SSD takes a few weeks to recover, to about January 5, 1996, although it still shows some occasional noise bursts. By early February 1996 the D1A SSD becomes extremely noisy, and it is not likely that the SSD will recover. This may be caused partly by radiation damage, since the D1 dome is only 0.0294 g/cm<sup>2</sup> thick aluminum.

#### 4.3 In-Orbit Dose and Flux Measurements

Samples of the PASP Plus dosimeter data taken shortly after launch were shown in Reference 1. At launch the APEX spacecraft was in an elliptical orbit with apogee and perigee in the equatorial plane. This results in the apogee being near the center of the inner radiation belt of high-energy protons. A typical plot of the uncorrected flux counts from the D1A, D2B, D3 and D4 detectors is shown in Figures 9 to 12. The data cover slightly more than three full orbits starting from 0556:44 UT on August 7, 1994, with data from four apogees being shown. Note that the apogee data show some variation in the peak flux counts, which is a result of the offset of the earth's magnetic dipole from the earth's center of mass. The pattern has a 24 hour period as the earth rotates under the spacecraft orbit.

The data in Figures 9 to 12 show the pattern from high energy proton fluxes in the thicker domes, with D2B, D3 and D4 showing significant counts in the LOLET, HILETA and HILETB counts at the apogee peaks. The D1A dome shows most of the counts at the apogee peak coming from the LOLET channel, which comes mostly from lower energy electrons (<1 MeV). The D1B detector shows a count pattern similar to the D1A detector, except that the counts are about a factor of 5 higher and the dead time effects are greater. The D2A detector has counts about a factor of 5 lower than the D2B detector; since neither the D2A nor D2B detectors have significant dead time effects, the D2B data are shown since the statistical accuracy is better. Note that the D1A detector LOLET flux has a significant dead time at the inner belt peak, and this accounts for the flattening of the plotted data. For the D2B, D3 and D4 detectors the sum of LOLET + HILETA + HILETB is nearly equal to the TOTAL count, since the dead time effects are small (see Table 6 and the discussion in Section 2.2).

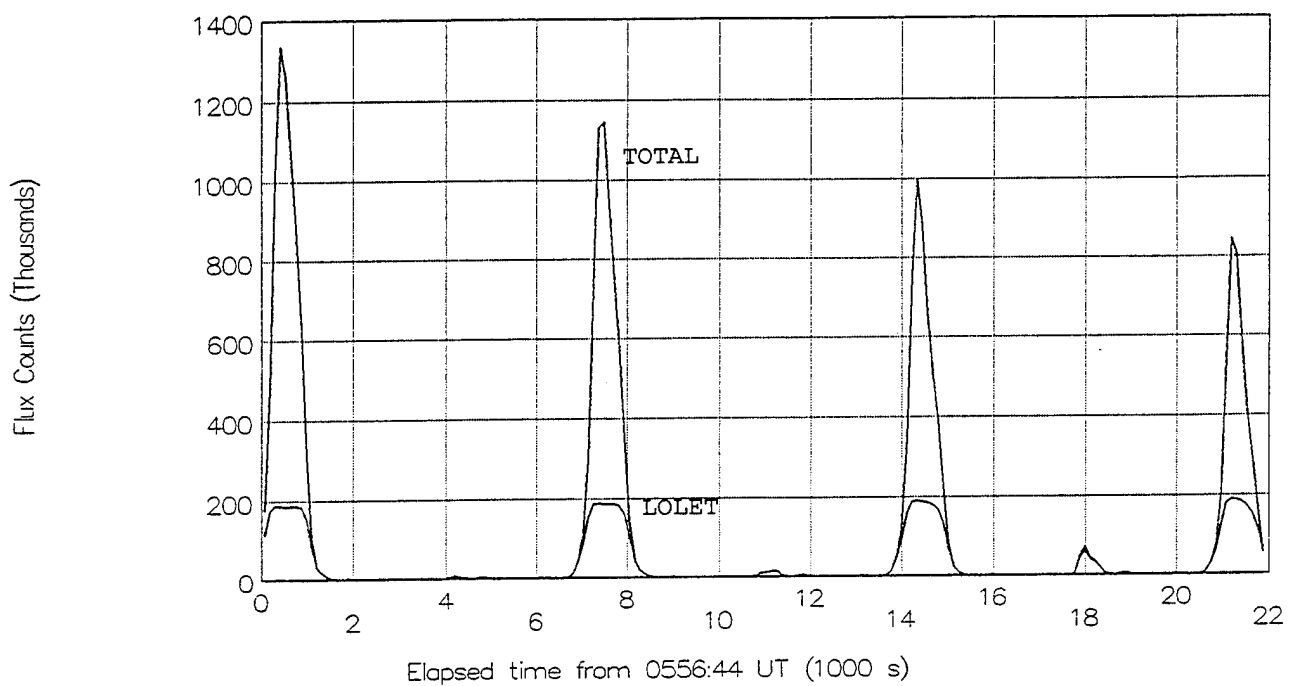


Figure 9. Dosimeter D1A Channel Counts for August 7, 1994.

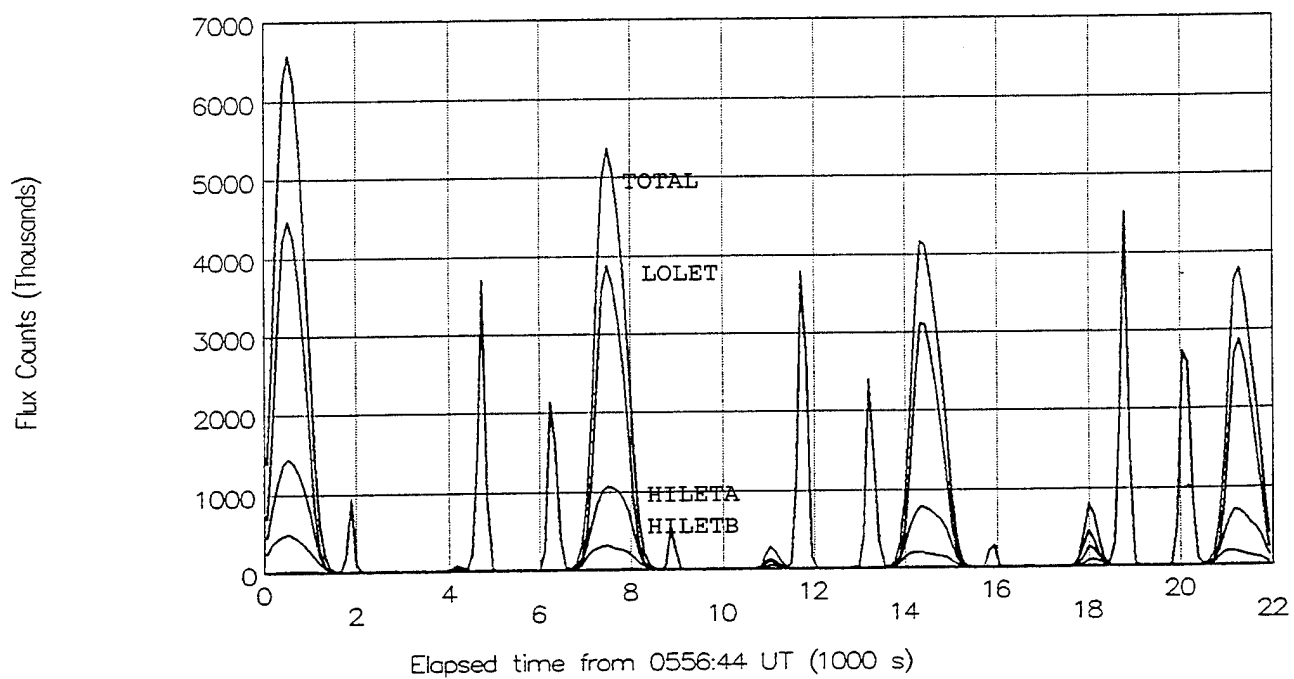


Figure 10. Dosimeter D2B Channel Counts for August 7, 1994.

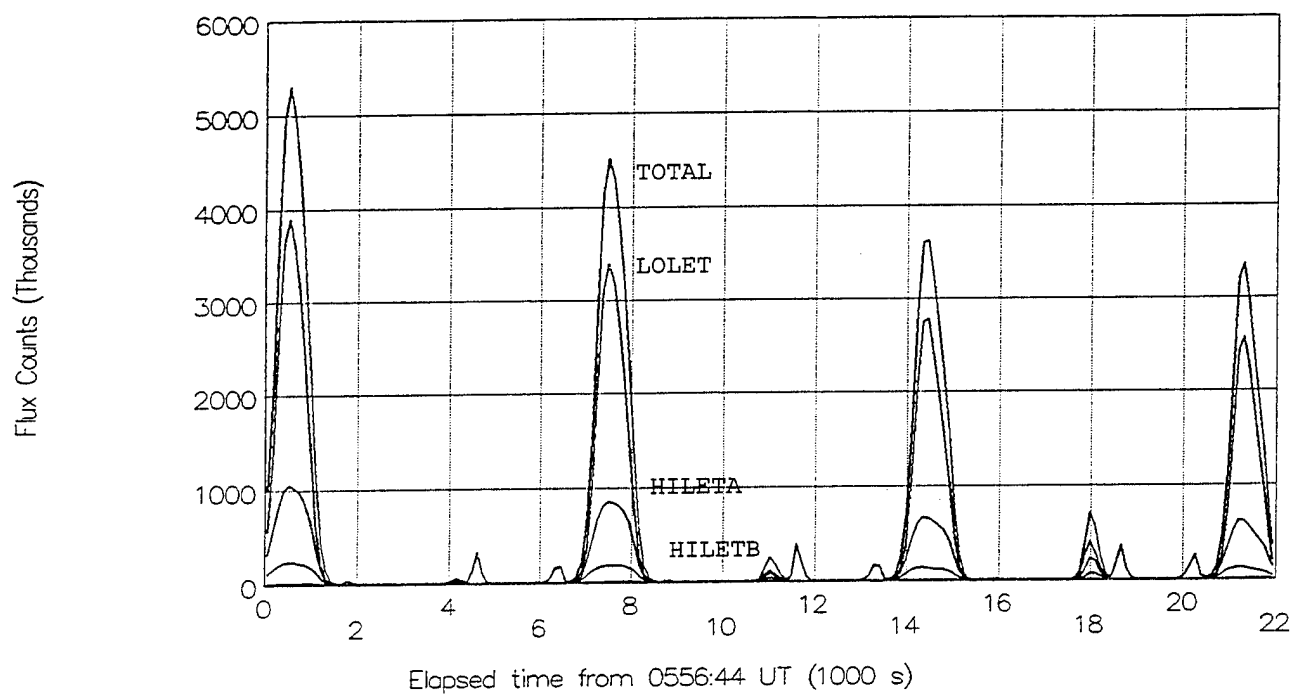


Figure 11. Dosimeter D3 Channel Counts for August 7, 1994.

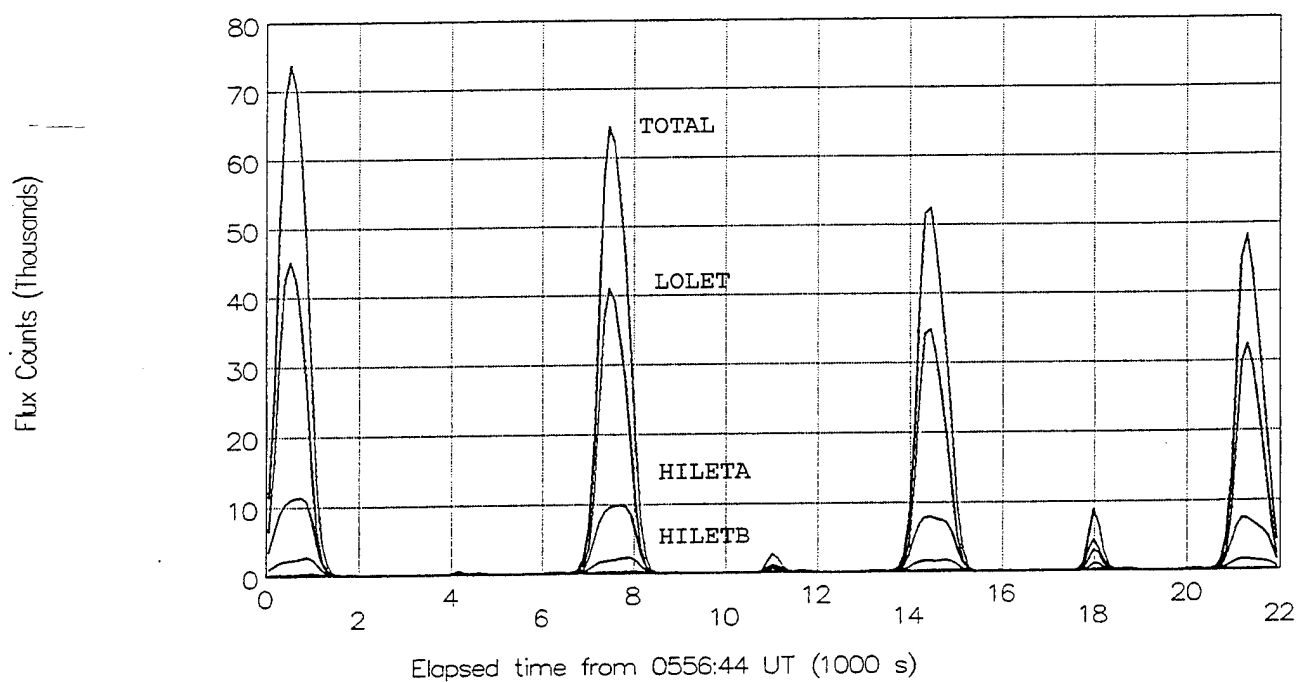


Figure 12. Dosimeter D4 Channel Counts for August 7, 1994.

PASP Plus dosimeter flux data from a few months after launch are shown in Figure 13 to 16. These data are for the D1A, D2B, D3 and D4 doses for about 5 full orbits starting from 1439:35 UT on November 2, 1994. By this time the APEX spacecraft apogee had rotated in its orbits plane so that it occurred away from the earth's equator, and the dosimeter was now obtaining a significant sample from the outer radiation belt. This is illustrated best by the D2B data shown in Figure 14, where the inner belt is shown by the peaks in LOLET, HILETA and HILETB, while the outer belt is shown by a peak which is mostly in the LOLET channel. Note that the outer zone peaks are much weaker in the D3 and D4 plots of Figures 15 and 16, indicating an electron spectrum that falls off significantly between 1 MeV and 2.5 MeV. The peak flux count rates for the inner belt shown in Figures 13 to 16 are comparable to those shown in Figures 9 to 12. The variation of the peak count rates with orbit are also shown, an effect caused by the offset of the earth's magnetic dipole from the center of mass.

The dosimeter dose measurements for the two periods discussed above are summarized below in Tables 17 and 18. Note that the doses do not have the dead-time correction of Eq. (2.4) applied, so the D1A and especially the D1B doses are somewhat low. From Table 6 it can be seen that the D1A dose is low by less than about 10%, while the D2B dose may be low by more than 30%. The B/A dose ratios of Tables 17 and 18 are in agreement with these estimates.

Table 17: Average Dose Rates for August 7, 1994

Channel	LOLET Doses		HILET Doses		Total Doses		Ratio (B/A) (Total)
	<u>Rad</u> orbit	<u>Rad</u> day	<u>Rad</u> orbit	<u>Rad</u> day	<u>Rad</u> orbit	<u>Rad</u> day	
D1A	622.4	7783.	11.77	147.2	634.2	7930.	0.70
D1B	436.5	5459.	9.97	124.7	446.5	5583.	
D2A	1.485	18.57	3.99	49.9	5.48	68.5	0.96
D2B	1.133	14.16	4.10	51.3	5.23	65.4	
D3	0.649	8.12	1.86	23.2	2.51	31.3	-
D4	0.484	6.05	1.08	13.5	1.57	19.6	-

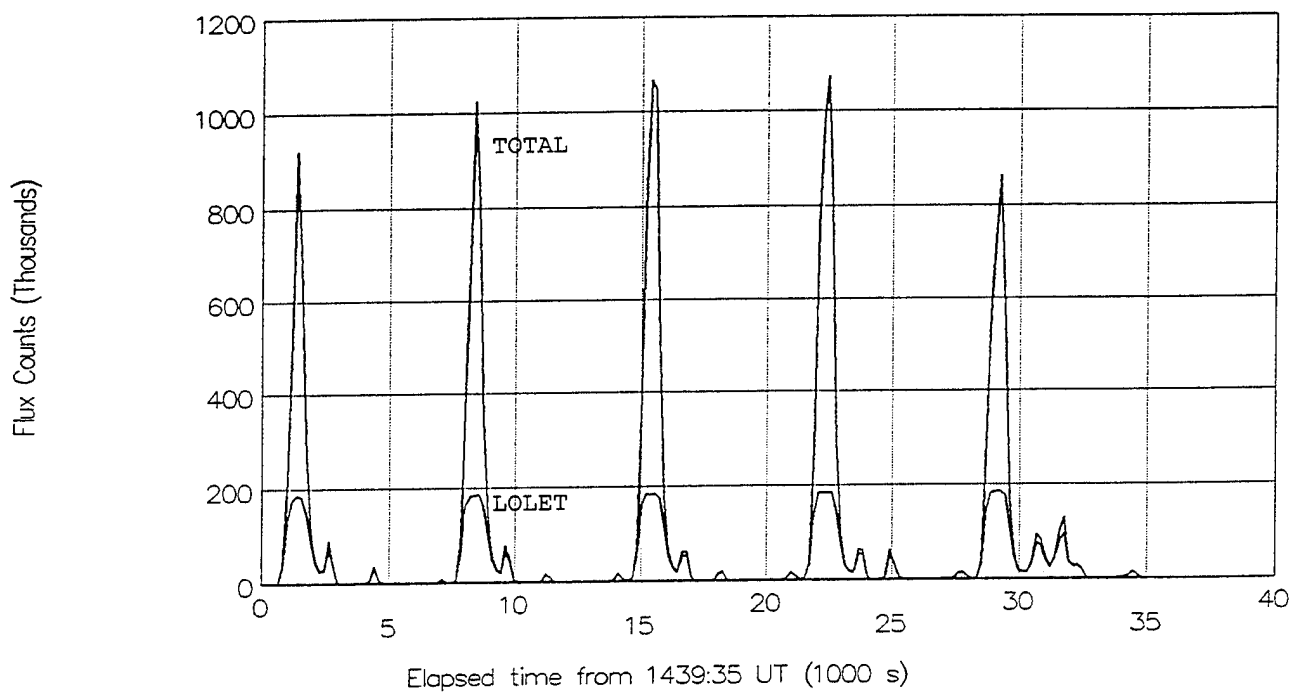


Figure 13. Dosimeter D1A Channel Counts for November 2, 1994.

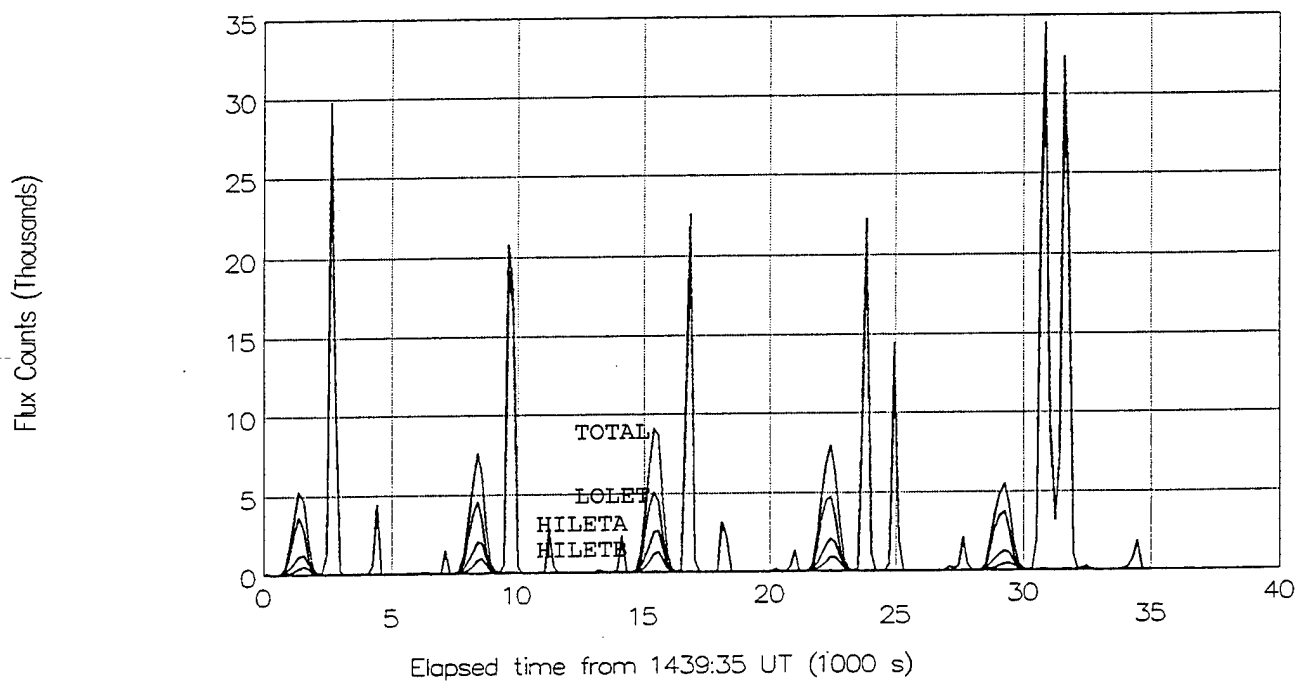


Figure 14. Dosimeter D2B Channel Counts for November 2, 1994.



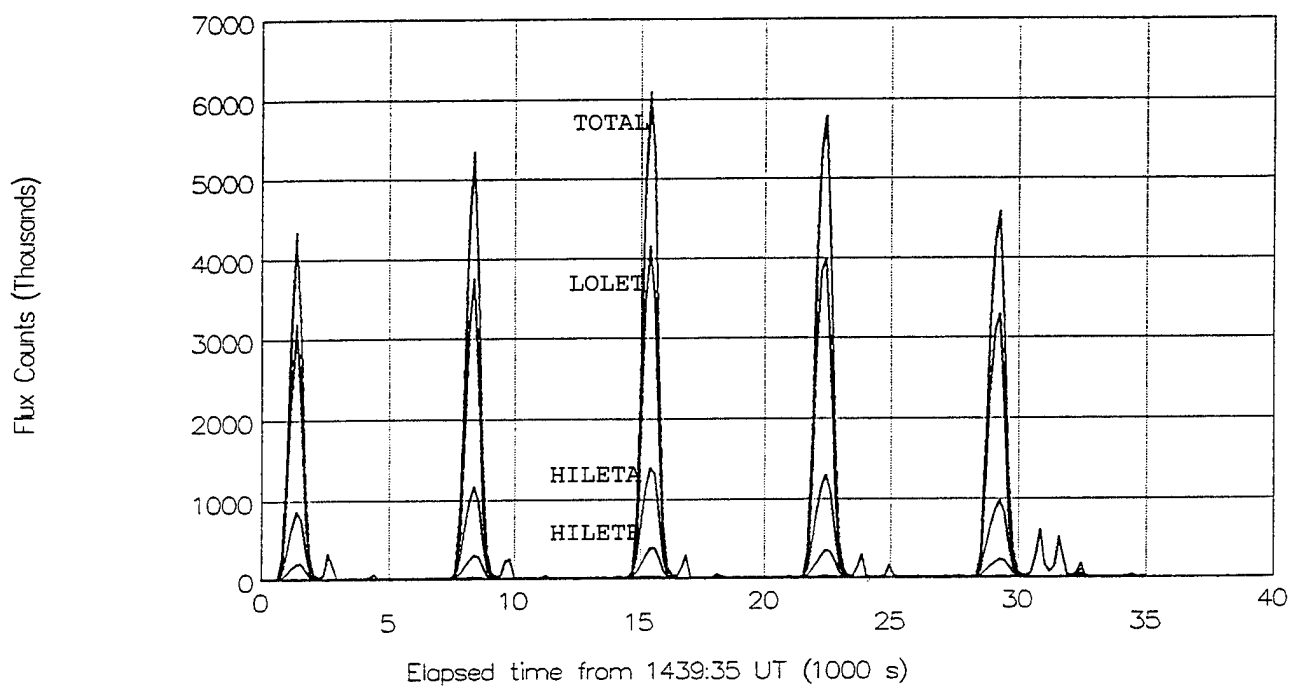


Figure 15. Dosimeter D3 Channel Counts for November 2, 1994.

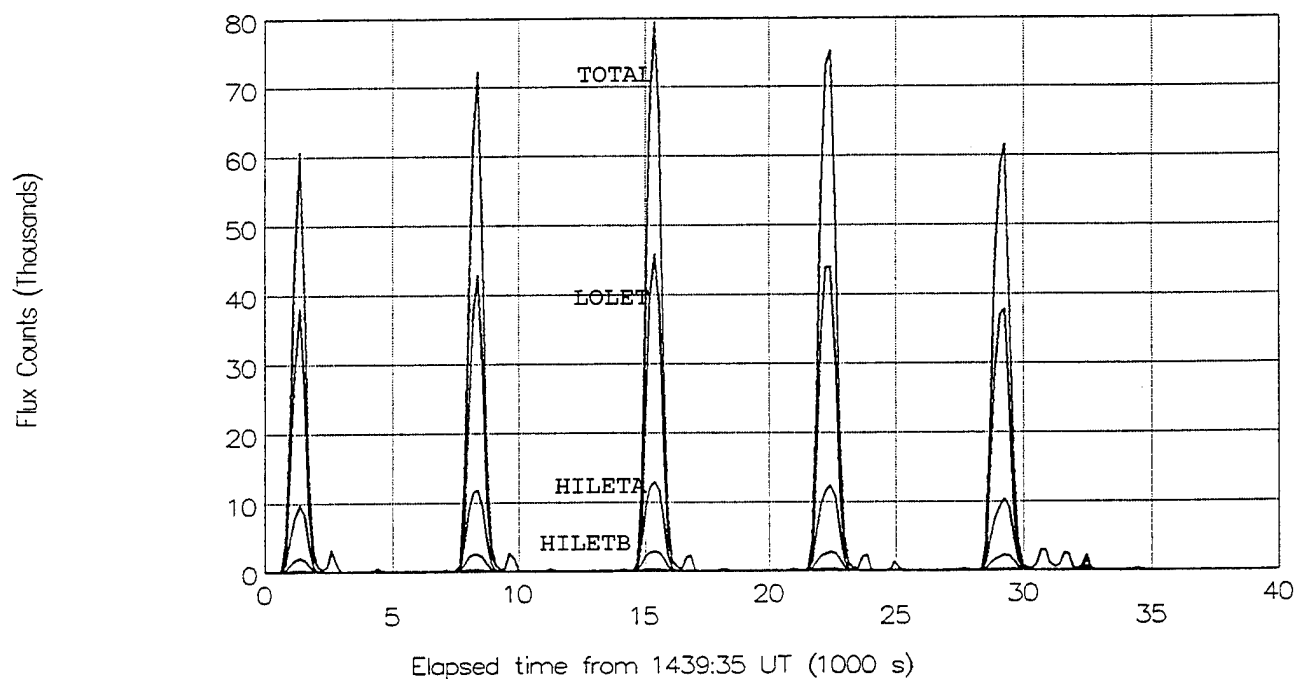


Figure 16. Dosimeter D4 Channel Counts for November 2, 1994.

Table 18: Average Dose Rates for November 2, 1994

Channel	LOLET Doses		HILET Doses		Total Doses		Ratio (B/A) (Total)
	<u>Rad</u> orbit	<u>Rad</u> day	<u>Rad</u> orbit	<u>Rad</u> day	<u>Rad</u> orbit	<u>Rad</u> day	
D1A	317.2	3973.	5.32	66.57	322.5	4040.	0.86
D1B	272.1	3408.	5.11	64.02	277.2	3472.	
D2A	1.975	24.74	1.790	22.42	3.765	47.16	0.98
D2B	1.890	23.67	1.787	22.39	3.677	46.06	
D3	0.392	4.91	0.960	12.02	1.352	16.93	-
D4	0.303	3.80	0.599	7.50	0.902	11.30	-

## 5. Summary and Conclusions

Two dosimeters have been fabricated for use on the APEX satellite, with the dosimeter SN/2 installed as part of the PASP Plus payload. The launch of the APEX spacecraft took place on 3 August 1994. The PASP Plus dosimeter provides six (6) channels for dose measurement under four (4) thicknesses of aluminum shielding. The two thinnest aluminum shields have two detectors of different sizes to allow for a larger dynamic range in particle flux. The nominal electron threshold energies of the four domes (range-energy table calculations) are 0.15 MeV, 1.0 MeV, 2.5 MeV and 5.0 MeV.

The dosimeter SN/1 was calibrated with electrons at an MIT Van de Graaff accelerator. Measurements were made with effective electron energies of 0.169 MeV to 3.076 MeV. The low-energy data are in disagreement with earlier calibration data for the CRRES and DMSP/F7 dosimeters, but the newer electron calibration data are believed to be the more accurate. The calibration data have been reduced to provide electron geometric factors for the LOLET and HILETA channels of the lower-energy domes.

The in-orbit operation of the dosimeter on APEX has been excellent, with dose data being provided for all four domes. After one year 9 months in orbit the PASP Plus dosimeter SN/2 was still operating properly.

## References

1. P. R. Morel, F. Hanser, J. Belue and R. Cohen, "Develop and Fabricate a Radiation Dose Measurement System for Satellites", Report PL-TR-94-2277 (November 1994), ADA295137.
2. F. A. Hanser and P. R. Morel, "Analyze Data from the PASP Plus Dosimeter on the APEX Spacecraft", Report PL-TR-95-2133 (22 September 1995), ADA301488.
3. M. S. Gussenhoven, E. G. Mullen, R. C. Filz, F. A. Hanser and K. A. Lynch, "Space Radiation Dosimeter SSJ\* for the Block 5D/Flight 7 DMSP Satellite: Calibration and Data Presentation", Report AFGL-TR-86-0065 (20 March 1986), ADA172178.
4. B. K. Dichter and F. A. Hanser, "Development and Use of Data Analysis Procedures for the CRRES Payloads AFGL-701-2/Dosimeter and AFGL-701-4/Fluxmeter and Application of the Data Analysis Results to Improve the Static and Dynamic Models of the Earth's Radiation Belts", Report PL-TR-92-2066 (March 1992), ADA253287.